

# Photocleavable Dimerizer for the Rapid Reversal of Molecular Trap Antagonists\*

Received for publication, August 24, 2013, and in revised form, December 19, 2013  
Published, JBC Papers in Press, January 13, 2014, DOI 10.1074/jbc.C113.513622

Shubbir Ahmed<sup>1</sup>, Jun Xie<sup>1</sup>, David Horne, and John C. Williams<sup>2</sup>

From the Department of Molecular Medicine, Beckman Research Institute of City of Hope, Duarte, California 91010

**Background:** The ability to rapidly turn on and off an acute antagonist is helpful to understand the initiation of a cellular program.

**Results:** A photocleavable analog was produced and functionally demonstrated.

**Conclusion:** Fine temporal control of endosome dispersion and restoration was obtained.

**Significance:** The combination of traps and the photocleavable analog permits new avenues to study signaling within a single cell in an organism.

Herein, we report the development of a photocleavable analog of AP20187, a cell-permeable molecule used to dimerize FK506-binding protein (FKBP) fusion proteins and initiate biological signaling cascades and gene expression or disrupt protein-protein interactions. We demonstrate that this reagent permits the unique ability to rapidly and specifically antagonize a molecular interaction *in vitro* and follow a biological process due to this acute antagonism (*e.g.* endosome dispersion) and to release the trap upon photocleavage to follow the cell's return to homeostasis. In addition, this photocleavable AP20187 analog can be used in other systems where the dimerization of FKBP has been used to initiate signaling pathways, offering the ability to correlate the duration of a signaling event and a cellular response.

The ability to rapidly and specifically regulate the activity of selected proteins and macromolecular complexes is essential to parse out critical functions in complicated macromolecular systems (*e.g.* signal transduction, protein trafficking, cell division) (1, 2). In combination with functional assays such as imaging, immunoprecipitation, Western blot analysis, RT-PCR, etc., perturbing the function of specific proteins of interest can reveal novel associations, critical post-translation modifications, and upstream and downstream effectors. Although small molecule inhibitors exist that lend themselves to such analyses (*e.g.* protein kinase, histone deacetylase, protease, and G protein-coupled receptor inhibitors), the actions of most of these

inhibitors are primarily focused on a small subset of enzymes that are frequently therapeutic targets. In fact, only 2% of all predicted human gene products (mostly kinases) have been successfully targeted with small molecules, and it is estimated that only 10–15% of the human genome is “druggable” (3). Thus, there is a tremendous gap in that only a handful of gene products can be studied using small molecule inhibitors, whereas there is a paucity of useful inhibitors for the remaining 85–90% of gene products.

The limited number of novel small molecule inhibitors stems from multiple sources and is partially because a large number of gene products act as components of macromolecular complexes and bind to their respective target(s) through extended surface contacts. The binding affinity and specificity for these interactions arise through multiple weak interactions, and the protein targets frequently lack a deep, solvent-occluded cleft as is typically found in enzymes (4, 5). Moreover, many proteins share common domains, and thus potential inhibitors may target a common domain and therefore could lack the required specificity and produce off-target effects.

To address this issue and leverage the specificity and affinity inherent in protein-protein interactions, yet maintain the advantages of small molecule antagonists, we recently developed chemically induced molecular traps that use the cell-permeable, small molecule AP20187 (hereafter referred to as AP)<sup>3</sup> to dimerize FKBP-peptide fusions to create high affinity, bivalent “ligands” that rapidly agonize specific targets (6) (see Fig. 1A). We demonstrated that the expression and subsequent dimerization of a dynein light chain LC8 or TcTex1 molecular trap immediately affects dynein-associated processes (*e.g.* endosome, lysosome, and Golgi dispersion) (6). The ability to reverse this perturbation would provide additional, powerful insight to molecular processes that is not available with current technologies (*e.g.* siRNA or expression of a dominant negative construct). However, we could not “wash” out the chemical dimerizer, AP, and thus could not reverse the perturbation to the system and follow its return to homeostasis. To address this shortcoming, we have created a photocleavable version of AP (hereafter referred to as PhAP) that, upon cleavage, reduces the valency of the trap, frees the targeted endogenous ligand, and permits one to disrupt a biochemical process and follow its return to equilibrium.

## EXPERIMENTAL PROCEDURES

**Synthesis of PhAP**—To a stirred solution of diol (9.5 mg, 0.045 mmol, 1 eq) in CH<sub>2</sub>Cl<sub>2</sub> (2 ml) were added acid (70 mg, 0.1 mmol, 2.2 eq) and catalysts 4-dimethylaminopyridine and *N,N*-dicyclohexylcarbodiimide (24 mg, 0.12 mmol, 2.6 eq) at room temperature. After 20 h, the solid was removed through filtration, and the filtrate was concentrated in vacuum. The residue was purified by silica gel column chromatography (40–60% EtOAc/hexane) to

\* This work was supported, in whole or in part, by National Institutes of Health Grant R21NS071166 (to J. C. W.) and National Institutes of Health Grant P30CA033572 from the NCI (to Michael A. Friedman).

<sup>1</sup> Both authors contributed equally to this work.

<sup>2</sup> To whom correspondence should be addressed: Dept. of Molecular Medicine, Beckman Research Institute of City of Hope, 1710 Flower Ave., Duarte CA 91010. E-mail: jcwilliams@coh.org.

<sup>3</sup> The abbreviations used are: AP, AP20187; PhAP, photocleavable AP analog; FKBP, FK506-binding protein; EGFP, enhanced green fluorescent protein; IC, intermediate chain.

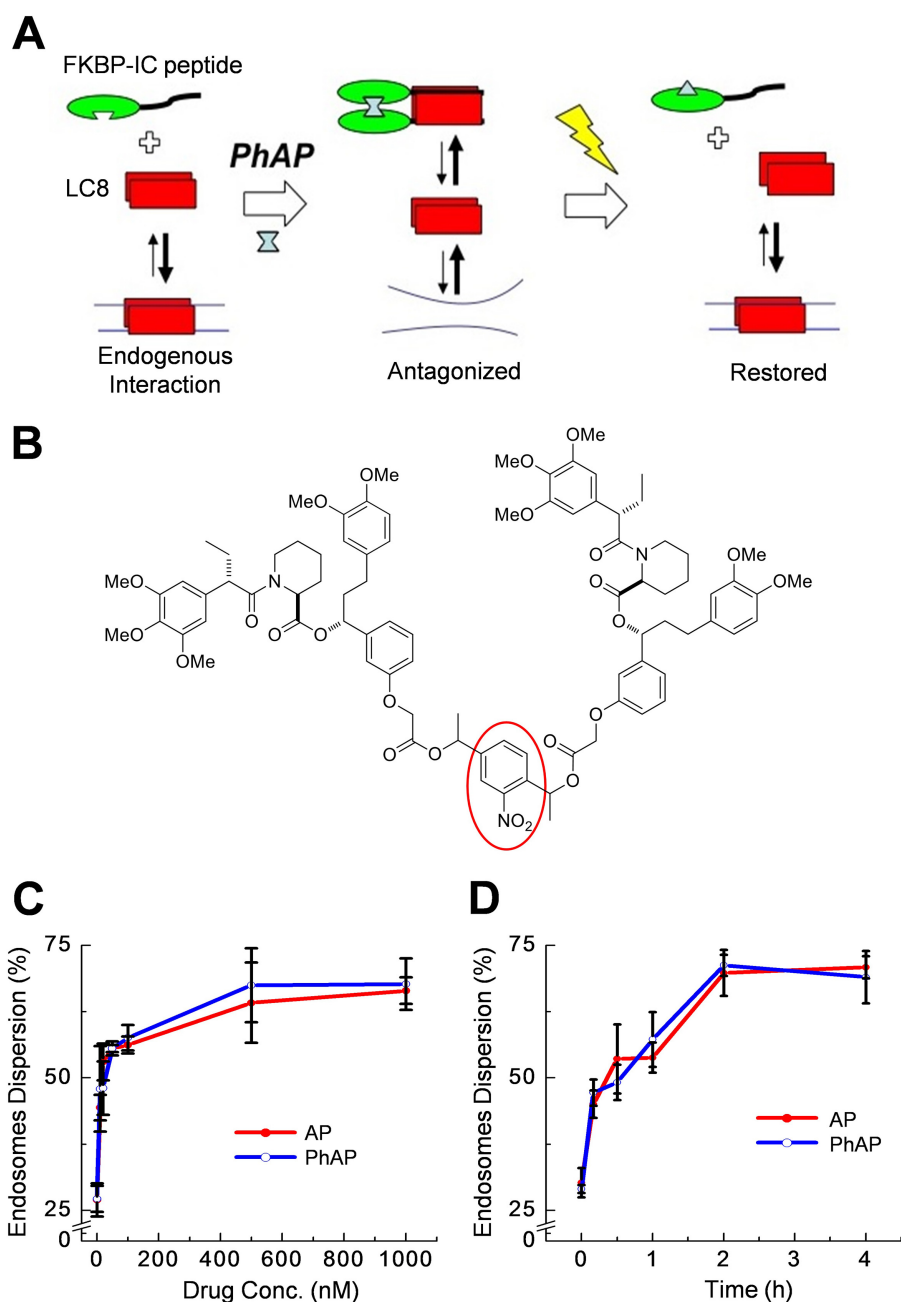


**FIGURE 1. Molecular trapping uses the chemically induced dimerization of FKBP to create a bivalent, high affinity ligand to either sequester an endogenous protein or directly antagonize an interface.** *A*, schematic presentation of the trapping mechanism. The dynein intermediate chain (IC) peptide, which binds to LC8 with low affinity as a monomer, is fused to FKBP (green), which binds to LC8 (red), competes with endogenous ligands (IC, blue lines), and induces phenotypes associated with dynein antagonism (e.g. endosome dispersion). The multivalent complex is highly stable. *B*, the PhAP with a nitrobenzyl moiety (shown in the oval). Creation of a photocleavable dimerizer (PhAP) will facilitate the dissociation and reverse the antagonism after exposure to UV light. *C*, endosome dispersion as a function of concentration of AP/PhAP. EGFP-FKBP-LC8<sub>TRAP</sub> transfected COS1 cells were treated with different concentrations of AP (red) or with PhAP (blue) for 2 h. Both AP and PhAP showed the same effect on endosome dispersion as a function of concentration. Maximum dispersion is seen with 500 nM of drug concentration and remains unchanged with further increase in drug concentration. *D*, endosome dispersion as a function of time. EGFP-FKBP-LC8<sub>TRAP</sub> transfected COS1 cells were treated with 500 nM AP (red) or with PhAP (blue) for different times. Both AP and PhAP showed the same time dependence on endosome dispersion. Maximum dispersion was reached after 2 h of drug treatment and remained unchanged with further increase in time. In each case cells were fixed and stained for early endosome marker (EEA1) and 100 cells were counted for endosome dispersion. Each experiment was repeated in triplicate ( $n = 3$ ). Error bars indicate mean  $\pm$  S.E.

afford the product (70 mg, 70%). High resolution mass spectrometry  $C_{86}H_{103}N_3O_{24}$   $[M+Na]^+$  calculated 1584.6824, found 1584.6830.

**Construction of Expression Plasmids**—Both the LC8 and the FKBP-LC8<sub>TRAP</sub> were cloned in bacterial expression vector (pET21D), expressed, and purified as described previously (6).

For EGFP-tagged FKBP-LC8<sub>TRAP</sub>, the construct was cloned as a C-terminal fusion of enhanced green fluorescence protein (EGFP) mammalian expression vector (pEGFPC1; Clontech) as described previously (6).

**Native PAGE**—Both LC8 and FKBP-LC8<sub>TRAP</sub> were mixed in a molar concentration of 50  $\mu$ M and 1.2 molar excess (60  $\mu$ M) of AP

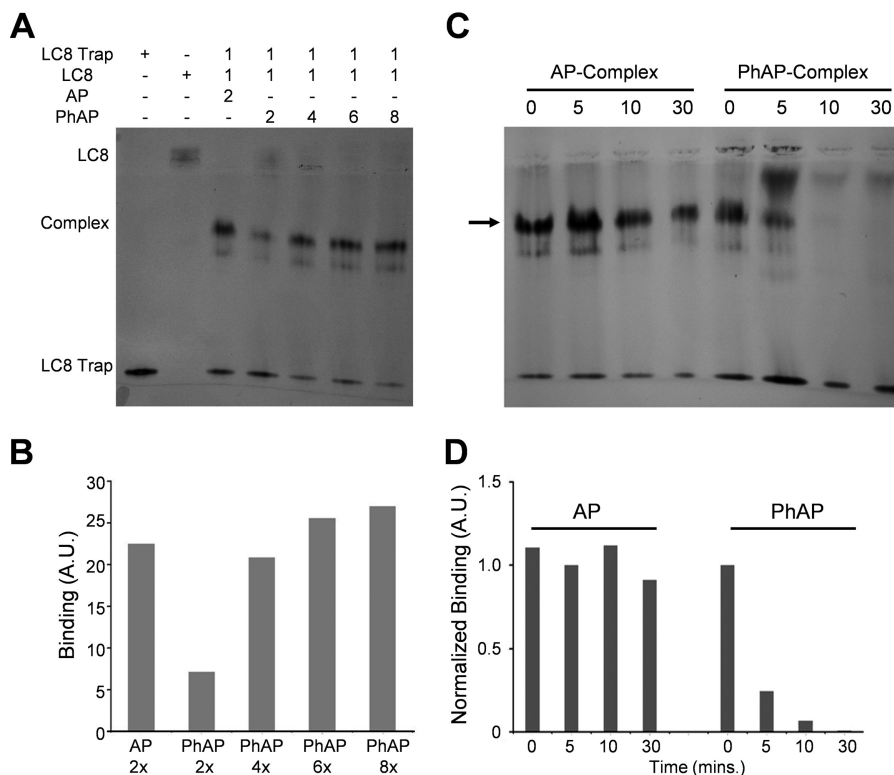


FIGURE 2. Native PAGE analysis of LC8-LC8<sub>TRAP</sub> complex formation and their dissociation on UV induction. **A**, native PAGE analysis of PhAP activity. LC8 migrates near the front of the gel. The LC8 trap monomer (*i.e.* FKBP-IC peptide) is positively charged and does not enter the gel. A complex forms when a mix of equimolar concentration of LC8 and LC8<sub>TRAP</sub> is treated with different molar concentrations of AP or PhAP (1×, 2×, etc.). **B**, quantification of the band intensities from **A**. **C**, native PAGE analysis of LC8-LC8<sub>TRAP</sub> complexes formed using AP or PhAP and exposed to UV light (365 nm) for the indicated times (min). **D**, intensity ratio of the complex band versus the LC8 band as a function of UV exposure.

or 2.4 molar excess (120 μM) of PhAP. The mix was incubated at 4 °C for 5 min. Native PAGE analysis was performed at 16 °C using 8–25% gradient gels on the Phast system (GE Healthcare).

**Antibodies and Reagents**—Anti-EEA1 monoclonal antibody was purchased from BD Biosciences, rhodamine-conjugated donkey anti-mouse secondary antibody was from Millipore, mounting medium Permount was from Fisher Scientific, 37% formaldehyde was from Sigma, Lipofectamine 2000 was from Invitrogen, Opti-MEM medium was from Gibco (Life Technologies), and DMEM medium and 10× PBS were from Cellgro.

**Cell Culture**—COS1 cells were cultured in DMEM (Cellgro) supplemented with 10% fetal bovine/calf serum (Omega Scientific). Transfection was performed in 80–90% confluent 24-h cultures of COS1 cells using Lipofectamine 2000 (Invitrogen) and Opti-MEM medium (Gibco; Life Technologies) according to the manufacturer’s recommendations. Various concentrations (0–1000 nM) of AP (Ariad Pharmaceuticals Inc.) and PhAP (synthesized by us) were added to each experimental well 24 h after transfection and incubated for different periods of time before analyzing the cells. For reversibility of endosome dispersion studies, 500 nM AP/PhAP was used. In each case, the cells were washed well with PBS, supplemented with fresh medium before inducing with UV light (10 min, 365 nm, 4 watts), and allowed to recover for various time periods at 37 °C before analysis.

**Immunostaining and Microscopy**—For immunostaining, transiently transfected COS1 cells were fixed with 3.7% form-

aldehyde at room temperature for 10 min, and subsequent immunostaining was performed as described previously (6). Briefly, COS 1 cells grown on 25-mm coverslips were washed three times with PBS, treated with 3.7% formaldehyde (Sigma) in PBS for fixation, and permeabilized in 0.5% Triton X-100 (Sigma) in PBS at room temperature for 10 min. Cells were then incubated with blocking buffer containing 4% skimmed milk (fat-free) and 0.5% Triton X-100 in PBS. Anti-EEA1 monoclonal antibody was added to label early endosome marker protein at a dilution of 1:100 in the same buffer for 30 min at room temperature, and the coverslips were washed and incubated with rhodamine-conjugated donkey anti-mouse secondary antibody (1:100). After washing, the coverslips were mounted on slides to visualize the trapping effects. Samples were viewed using an Olympus IX81 automated inverted microscope equipped with a water immersion ×60 objective. The level of dispersion was quantified by counting 100 cells per coverslip. We considered a cluster of EEA1-stained endosomes at the perinuclear region as “compact” (see Fig. 3B), whereas endosomes spread throughout the cell were considered as “dispersed” (see Fig. 3B). Each experiment was performed in triplicate. Images were obtained using a Spot RT Slider high-resolution cooled CCD camera equipped to an IX81 microscope and Image-Pro software. Images were cropped and processed using Adobe Photoshop 7.0 (Adobe Systems), unless otherwise noted.

**UV Induction**—For UV induction and recovery of endosome studies, cells were washed with PBS, and fresh medium was added. The washed cells were then treated with a hand-held UV lamp (365 nm/4 watts) for 10 min by holding the UV lamp 2 cm above the coverslip containing the cells. The cells were then left to recover at 37 °C for varying periods of time before staining and analysis.

**ImageJ (NIH) quantification**—For quantitative analysis of complex formation, we used ImageJ software from NIH. In each case, the software was used to quantify bands on the scanned PAGE.

## RESULTS

**Synthesis of PhAP**—First, we synthesized a UV-induced photolysable AP by replacing the amine linker of AP with a photocleavable *o*-nitrobenzyl moiety to create PhAP. This synthesis relied on the use of intermediate **5**, which was prepared as described previously (7). The final coupling between acid **5** and diol **6** (8) produced the photocleavable modulator PhAP (Fig. 1B).

**In Vitro Characterization of PhAP**—We tested whether the replacement of the amine linker with the *o*-nitrobenzyl moiety would affect the dimerization of FKBP *in vitro*. We used native PAGE to follow the formation of the LC8 and FKBP-LC8 molecular trap (LC8<sub>TRAP</sub>) complex induced by the addition of PhAP (6). Upon the addition of PhAP to an equimolar mixture of LC8 and LC8<sub>TRAP</sub>, we observed a new band of PhAP-LC8-LC8<sub>TRAP</sub> that migrated the same distance as the band produced by the addition of AP (AP-LC8-LC8<sub>TRAP</sub>) (Fig. 2A). Quantification of this new band indicated that a 2-fold higher concentration (2×) of PhAP was required to produce a band of the same intensity as the band produced by the sample treated with AP (Fig. 2B).

Next, we characterized how well UV light could disrupt the PhAP-LC8-LC8<sub>TRAP</sub> complex *in vitro*. We generated the PhAP-LC8-LC8<sub>TRAP</sub> and AP-LC8-LC8<sub>TRAP</sub> complexes and exposed each to UV light (365 nm/4 watts). Native PAGE indicated loss of the band corresponding to the PhAP-LC8-LC8<sub>TRAP</sub> complex and an increase in intensity of bands corresponding to the individual components after UV induction. The band corresponding to the PhAP-LC8-LC8<sub>TRAP</sub> complex was less intense in samples that received a 5-min exposure to UV light and undetectable after a 10-min exposure. On the other hand, the LC8-LC8<sub>TRAP</sub> complex induced by the non-photocleavable AP (AP-LC8-LC8<sub>TRAP</sub>) persisted, even after a 30-min exposure to UV light (Fig. 2C). A band intensity quantification of the ratio of the complex against the LC8 shows that the ratio remains unchanged in case of AP-LC8-LC8<sub>TRAP</sub>, whereas the same is undetectable after 10 min of UV exposure for PhAP-LC8-LC8<sub>TRAP</sub> (Fig. 2D).

**In Vivo Study of Reversal of Endosome Dispersion on UV Induction**—To determine whether these biochemical results had relevance in cells, we investigated whether photocleavage of PhAP could reverse the endosome dispersion phenotype induced by LC8<sub>TRAP</sub> and PhAP. Initially, we established that PhAP behaved in a similar manner in cells as AP. To this end, we used a green fluorescent protein (GFP) analog of the trap, EGFP-FKBP-LC8<sub>TRAP</sub>, to identify cells that expressed the trap.

**TABLE 1**  
Percentage of endosome dispersion after treatment with PhAP or AP

	AP (%)	PhAP (%)
<b>Drug concentration (nM)<sup>a</sup></b>		
0	26.9 ± 3.1	27.2 ± 2.5
10	44.4 ± 2.4	47.9 ± 8.1
20	53.0 ± 3.5	48.0 ± 5.0
50	55.5 ± 0.7	55.5 ± 1.3
100	56.2 ± 1.6	57.5 ± 2.4
500	64.1 ± 7.6	67.5 ± 7.0
1000	66.4 ± 2.5	67.7 ± 4.9
<b>Time (h)<sup>b</sup></b>		
0	30.2 ± 2.8	29.0 ± 8
0.167 (10 min)	45.0 ± 2.6	47.2 ± 2.5
0.5	53.6 ± 6.5	49.1 ± 3.3
1	53.8 ± 2.9	57.2 ± 5.2
2	69.8 ± 4.3	71.2 ± 2.0
4	70.9 ± 2.1	69.0 ± 4.9
<b>Recovery after 2-h drug treatment<sup>c</sup></b>		
0	69.1 ± 3.2	69.5 ± 2.4
1	68.9 ± 3.2	66.3 ± 3.2
2	70.7 ± 4.0	57.6 ± 2.6
4	69.5 ± 1.9	44.1 ± 2.3
8	70.3 ± 3.3	48.9 ± 3.9
<b>Recovery after 1-h drug treatment<sup>d</sup></b>		
0	58.0 ± 4.3	57.8 ± 8.0
1	71.2 ± 2.5	56.4 ± 1.7
2	69.7 ± 3.6	55.7 ± 8.8
4	70.4 ± 3.1	46.7 ± 0.6
8	70.8 ± 1.9	48.1 ± 2.0
<b>Recovery after 30-min drug treatment<sup>e</sup></b>		
0	51.8 ± 4.4	53.2 ± 2.4
1	64.7 ± 2.0	53.7 ± 4.0
2	68.3 ± 3.7	50.8 ± 2.3
4	69.8 ± 4.3	48.0 ± 0.5
8	67.9 ± 1.9	49.3 ± 6.7

<sup>a</sup> Percentage of endosome dispersion as a function of AP/PhAP concentration after 2 h of treatment.

<sup>b</sup> Percentage of endosome dispersion as a function of time with 500 nM AP/PhAP concentration.

<sup>c</sup> Percentage of endosome dispersion at different time points (showing recovery for PhAP), after 2 h of AP/PhAP treatment (500 nM).

<sup>d</sup> Percentage of endosome dispersion at different time point s (showing recovery for PhAP), after 1 h of AP/PhAP treatment (500 nM).

<sup>e</sup> Percentage of endosome dispersion at different time points (showing recovery for PhAP), after 30 min of AP/PhAP treatment (500 nM).

COS1 cells were transiently transfected with EGFP-FKBP-LC8<sub>TRAP</sub> for 24 h, after which they were treated with PhAP or AP (0 nM–1000 nM) for 2 h. Cells were then fixed and stained with an early endosome marker 1 (EEA1). The number of cells with dispersed endosomes after treatment with PhAP or AP was indistinguishable. The maximum number of cells with dispersed endosomes (67.5 ± 7.0% for PhAP and 64.1 ± 7.6% for non-photocleavable AP) was obtained at dimerizer concentrations greater than 500 nM (Fig. 1C, Table 1, first row). The number of cells with dispersed endosomes over the same time course was also similar using either dimerizing agent, and no changes were observed past 2 h (Fig. 1D, Table 1, second row). The values obtained for both AP and PhAP are also in agreement with our previous studies (6).

Next, we characterized the reversibility of endosome dispersion in COS1 cells upon UV-induced cleavage of PhAP. In these experiments, transiently transfected cells were incubated with PhAP or AP (500 nM) for times ranging from 0 to 2 h, after which cells were washed rapidly, replenished with fresh medium, and then exposed to UV light (10 min, 365 nm, 4 watts). The cells were then fixed at 0, 1, 2, 4, and 8 h after UV radiation, and the endosomes were imaged using fluorescence microscopy at ×60 magnification. We observed a gradual

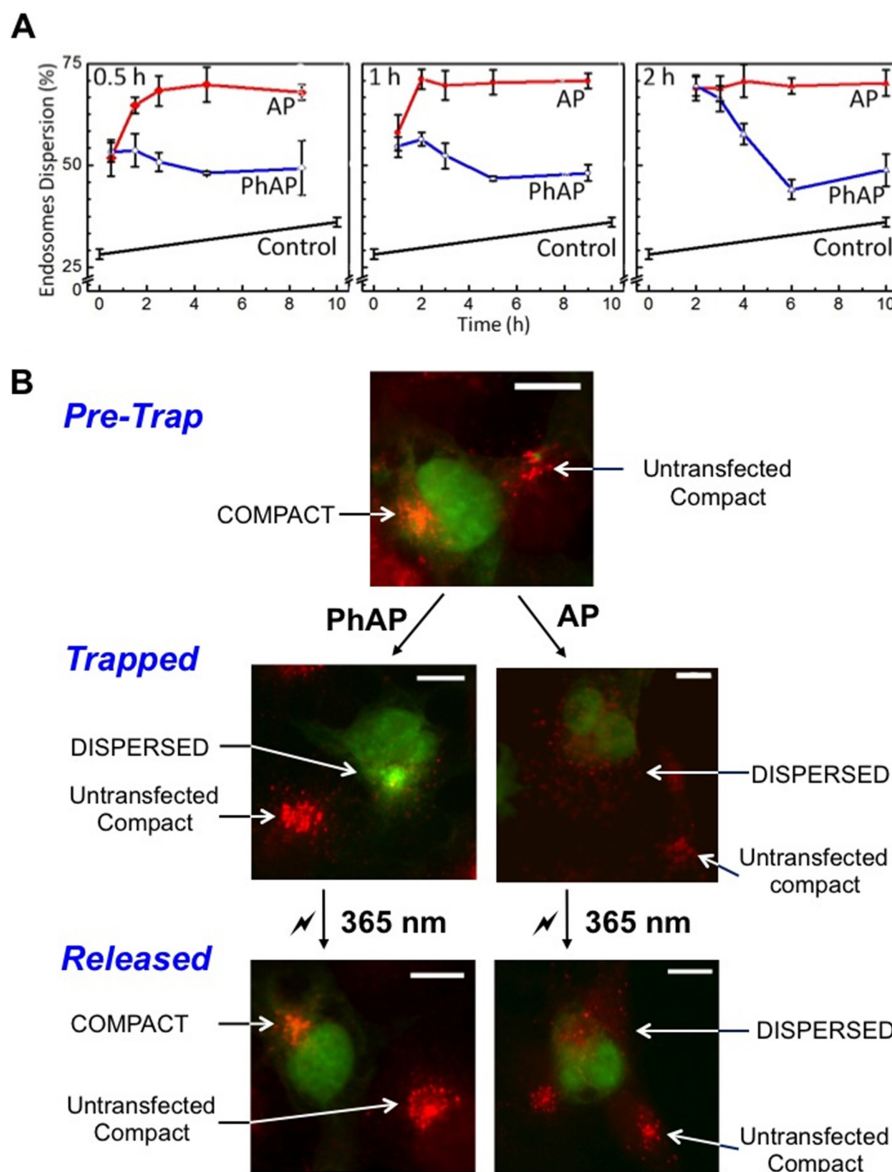


FIGURE 3. **Cell-based assays and quantification of endosome dispersion.** *A*, Cos1 cells were transiently transfected with EGFP-LC8<sub>TRAP</sub> and treated with AP (red) or PhAP (blue) for predetermined periods (0.5, 1, and 2 h), exposed to UV light, and then fixed and stained with fluorescently labeled anti-EEA1 antibody. Fluorescence microscopy was used to quantify the activity of the AP or PhAP on endosome dispersion. Each data point reflects 100 cells ( $n = 3$ ). Error bars indicate mean  $\pm$  S.E. *B*, endosome dispersion when treated with PhAP (right) or AP (left) as observed by fluorescence microscopy. Transfected cells harboring the trap are green (GFP fluorescence). The endosomes (red) in transfected cells disperse upon treatment with PhAP or AP. Upon UV treatment, endosomes in cells treated with PhAP return to their perinuclear location, whereas endosomes in cells treated with AP remain disperse. Note that endosomes in untransfected cells (no GFP) remain compact irrespective of the treatment and serve as a negative control.

recovery of endosomes to the perinuclear region during the first 4 h after UV exposure ( $44.1 \pm 2.3\%$ ), with a slight increase in dispersion after 8 h ( $48.9 \pm 3.9\%$ ), for cells treated with PhAP (Fig. 3A). On the other hand, when cells were treated with AP, the endosomes remained dispersed at all time points evaluated, regardless of whether they received UV exposure. As an internal control, cells that were not transfected (*i.e.* did not express GFP) were treated in the same manner. These cells showed a slight increase in endosome dispersion in 8 h after UV exposure. Of note, cells with compact endosomes 4 h after UV treatment did not return to the same percentage as before the addition of PhAP. However, this is not entirely unexpected because we typically observe that 20–25% of cells have dispersed endosomes, including the trap-bearing cells before

the addition of PhAP or AP, as well as cells not transfected with the trap. We also observed that a maximum of 70–75% of cells transfected with the trap had dispersed endosomes after treatment with PhAP or AP for 2 h. We suspect that incomplete recovery arises from several sources, including cell heterogeneity (9), effects of transient transfection, and the fact that cells were not synchronized throughout the experiment. However, similar spreads in these values have been reported in cell-based assays that used different methods to interfere with dynein-mediated processes, including RNAi (10, 11), expression of a dominant-negative protein (12), and/or microinjection of monoclonal antibodies (13), all of which are irreversible. Consistent with these results, in RNAi experiments targeting LC8, we observed that only 65%

of cells showed dispersion of the Golgi after 4 days of treatment as compared with 12% of cells exposed to a scrambled control.

Having established that photocleavage of PhAP reverses the phenotype, we asked whether the amount of time needed to restore perinuclear clustering of endosomes depended on how long the trap was allowed to act. As mentioned above, we found that maximal endosome dispersion occurred within 2 h, whereas the recovery occurred over a 4-h period. Thus, we treated cells for 30 min and 1 h with PhAP or AP followed by UV exposure. As expected, this resulted in a lower percentage of cells that had dispersed endosomes (0.5 h,  $53.2 \pm 2.4\%$ ; 1 h,  $57.8 \pm 8.0\%$ ; Table 1, fifth row). However, for all treatment times (0.5, 1, and 2 h), the percentages of cells with dispersed endosomes were similar within 4 h after exposure to UV light (Fig. 3A, Table 1). In contrast, cells treated exactly in the same manner, but with AP instead of PhAP, exhibited continued endosome dispersion until dispersion reached the saturation point ( $\sim 70\%$ ), further confirming that induction of the trap with AP creates a highly stable complex. Fig. 3B shows representative images of compact endosomes and their dispersion on AP/PhAP treatment. Please note that only transfected cells (*green*) show endosome dispersion (Fig. 3B, *DISPERSED*) and that untransfected cells, which act as an internal negative control, do not show endosome dispersion (Fig. 3B, *Untransfected compact*). However, in the case of PhAP, the endosomes return to their perinuclear position (Fig. 3B, *COMPACT*) upon UV irradiation. This is not the case for cells treated with AP where the dimeric trap remains associated and endosomes continue to disperse.

## DISCUSSION

Herein, we have developed a photocleavable analog of AP, demonstrated that PhAP can induce formation of the LC8-LC8<sub>TRAP</sub> complex, and shown that photocleavage of PhAP within this molecular trap leads to dissociation and rapid reversal of endosome dispersion. We also observed the time needed for endosomes to return to the perinuclear space was similar despite the treatment time. We note that these values reflect changes averaged over a large number of cells and that detailed mechanistic insight into this process will require live cell imaging (*e.g.* following endosome dispersion in individual cells before, during, and after cleavage of PhAP). Now that we have established the reversibility of the PhAP-mediated trap, we have initiated such mechanistic studies, not only following endosomes but also other organelles with the LC8 trap as well as using other molecular traps recently developed in the laboratory.

Finally, although we have applied this new reagent in the context of molecular trapping (6), dimerization of FKBP has also been used in many other systems, typically to induce a signal cascade (14–18), but also to oligomerize amyloid precursor protein (18–20) and as a “death switch” for cell-based therapies (21). It is likely that PhAP will be of value to these studies as well. Of note, a photocleavable rapamycin analog was recently created to dimerize FKBP and FKBP12-rapamycin-associated protein (FRAP). In this case, the photocleavage was used to activate the rapamycin analog for spatial and temporal

activation of the signaling event (22, 23). We propose that the PhAP presented herein, in conjunction with a molecular trap expressed by a tissue-specific promoter, will not only afford spatial and temporal activation of a biological process in an animal model (*e.g. Caenorhabditis elegans*), but also the ability to reverse a phenotype and address questions such as the period of a signal and commitment to a program that determines the fate of the cell.

*Acknowledgments*—We thank current and former members of the Williams and Horne laboratory for useful discussion. We also thank Professor Jim Keen at Thomas Jefferson University for insightful discussion.

## REFERENCES

- Rothman, J. E. (2010) The future of Golgi research. *Mol. Biol. Cell* **21**, 3776–3780
- Brieke, C., Rohrbach, F., Gottschalk, A., Mayer, G., and Heckel, A. (2012) Light-controlled tools. *Angew Chem. Int. Ed Engl.* **51**, 8446–8476
- Dixon, S. J., and Stockwell, B. R. (2009) Identifying druggable disease-modifying gene products. *Curr. Opin. Chem. Biol.* **13**, 549–555
- Sugase, K., Dyson, H. J., and Wright, P. E. (2007) Mechanism of coupled folding and binding of an intrinsically disordered protein. *Nature* **447**, 1021–1025
- Uversky, V. N., Oldfield, C. J., and Dunker, A. K. (2005) Showing your ID: intrinsic disorder as an ID for recognition, regulation and cell signaling. *J. Mol. Recognit.* **18**, 343–384
- Varma, D., Dawn, A., Ghosh-Roy, A., Weil, S. J., Ori-McKenney, K. M., Zhao, Y., Keen, J., Vallee, R. B., and Williams, J. C. (2010) Development and application of *in vivo* molecular traps reveals that dynein light chain occupancy differentially affects dynein-mediated processes. *Proc. Natl. Acad. Sci. U.S.A.* **107**, 3493–3498
- Yang, W., Rozamus, L. W., Narula, S., Rollins, C. T., Yuan, R., Andrade, L. J., Ram, M. K., Phillips, T. B., van Schravendijk, M. R., Dalgarno, D., Clackson, T., and Holt, D. A. (2000) Investigating protein-ligand interactions with a mutant FKBP possessing a designed specificity pocket. *J. Med. Chem.* **43**, 1135–1142
- Piggott, A. M., and Karuso, P. (2005) 9-Hydroxyfurodysinin-O-ethyl lactone: a new sesquiterpene isolated from the tropical marine sponge *Dysidea arenaria*. *Molecules* **10**, 1292–1297
- Hastings, R. J., and Franks, L. M. (1983) Cellular heterogeneity in a tissue culture cell line derived from a human bladder carcinoma. *Br. J. Cancer* **47**, 233–244
- Palmer, K. J., Hughes, H., and Stephens, D. J. (2009) Specificity of cytoplasmic dynein subunits in discrete membrane trafficking steps. *Mol. Biol. Cell* **20**, 2885–2899
- Dixit, R., Levy, J. R., Tokito, M., Ligon, L. A., and Holzbaur, E. L. (2008) Regulation of dynactin through the differential expression of p150<sup>Glued</sup> isoforms. *J. Biol. Chem.* **283**, 33611–33619
- Zhapparova, O. N., Burakov, A. V., and Nadezhkina, E. S. (2007) The centrosome keeps nucleating microtubules but loses the ability to anchor them after the inhibition of dynein-dynactin complex. *Biochemistry* **72**, 1233–1240
- Palazzo, A. F., Joseph, H. L., Chen, Y. J., Dujardin, D. L., Alberts, A. S., Pfister, K. K., Vallee, R. B., and Gundersen, G. G. (2001) Cdc42, dynein, and dynactin regulate MTOC reorientation independent of Rho-regulated microtubule stabilization. *Curr. Biol.* **11**, 1536–1541
- Zlatic, S. A., Tornieri, K., L'Hernault, S. W., and Faundez, V. (2011) Clathrin-dependent mechanisms modulate the subcellular distribution of class C Vps/HOPS tether subunits in polarized and nonpolarized cells. *Mol. Biol. Cell* **22**, 1699–1715
- Baker, D. J., Wijshake, T., Tchkonina, T., LeBrasseur, N. K., Childs, B. G., van de Sluis, B., Kirkland, J. L., and van Deursen, J. M. (2011) Clearance of p16<sup>Ink4a</sup>-positive senescent cells delays ageing-associated disorders. *Nature* **479**, 232–236

## REPORT: Photocleavable Molecular Traps

- Pajvani, U. B., Trujillo, M. E., Combs, T. P., Iyengar, P., Jelicks, L., Roth, K. A., Kitsis, R. N., and Scherer, P. E. (2005) Fat apoptosis through targeted activation of caspase 8: a new mouse model of inducible and reversible lipodystrophy. *Nat. Med.* **11**, 797–803
- Gazdoui, S., Yamoah, K., Wu, K., Escalante, C. R., Tappin, L., Bermudez, V., Aggarwal, A. K., Hurwitz, J., and Pan, Z. Q. (2005) Proximity-induced activation of human Cdc34 through heterologous dimerization. *Proc. Natl. Acad. Sci. U.S.A.* **102**, 15053–15058
- Abdel-Azim, H., Zhu, Y., Hollis, R., Wang, X., Ge, S., Hao, Q. L., Smbatyan, G., Kohn, D. B., Rosol, M., and Crooks, G. M. (2008) Expansion of multipotent and lymphoid-committed human progenitors through intracellular dimerization of Mpl. *Blood* **111**, 4064–4074
- Béland, M., Motard, J., Barbarin, A., and Roucou, X. (2012) PrPC Homodimerization stimulates the production of PrPC cleaved fragments Pr<sup>PN1</sup> and Pr<sup>PC1</sup>. *J. Neurosci.* **32**, 13255–13263
- Roostaei, A., Côté, S., and Roucou, X. (2009) Aggregation and amyloid fibril formation induced by chemical dimerization of recombinant prion protein in physiological-like conditions. *J. Biol. Chem.* **284**, 30907–30916
- Di Stasi, A., Tey, S. K., Dotti, G., Fujita, Y., Kennedy-Nasser, A., Martinez, C., Straathof, K., Liu, E., Durett, A. G., Grilley, B., Liu, H., Cruz, C. R., Savoldo, B., Gee, A. P., Schindler, J., Krance, R. A., Heslop, H. E., Spencer, D. M., Rooney, C. M., and Brenner, M. K. (2011) Inducible apoptosis as a safety switch for adoptive cell therapy. *N. Engl. J. Med.* **365**, 1673–1683
- Umeda, N., Ueno, T., Pohlmeier, C., Nagano, T., and Inoue, T. (2011) A photocleavable rapamycin conjugate for spatiotemporal control of small GTPase activity. *J. Am. Chem. Soc.* **133**, 12–14
- DeRose, R., Pohlmeier, C., Umeda, N., Ueno, T., Nagano, T., Kuo, S., and Inoue, T. (2012) Spatio-temporal manipulation of small GTPase activity at subcellular level and on timescale of seconds in living cells. *J. Vis. Exp.* **61**, 3794